http://dx.doi.org/10.5012/bkcs.2013.34.7.2148

Effects of Fused Thiophene Bridges in Organic Semiconductors for Solution-Processed Small-Molecule Organic Solar Cells

Jae Kwan Lee,* Sol Lee,† and Suk Jin Yun

*Department of Chemistry Education, Chosun University, Gwangju 501-759, Korea. *E-mail: chemedujk@chosun.ac.kr*
†Department of Green Energy Engineering, Hoseo University, Chungnam 336-795, Korea
Received March 31, 2013, Accepted April 24, 2013

Three push-pull organic semiconductors, **TPA-Th$_3$-MMN** (**1**), **TPA-ThTT-MMN** (**2**), and **TPA-ThDTT-MMN** (**3**), comprising a triphenylamine donor and a methylene malononitrile acceptor linked by various π-conjugated thiophene units were synthesized, and the effects of the π-conjugated bridging unit on the photovoltaic characteristics of solution-processed small-molecule organic solar cells based on these semiconductors were investigated. Planar bridging units with extended π-conjugation effectively facilitated intermolecular π-π packing interactions in the solid state, resulting in enhanced J_{sc} values of the SMOSCs fabricated with bulk heterojunction films.

Key Words : Organic semiconductor, Fused thiophen, Intermolecular packing, Bulk heterojunction, Organic solar cell

Introduction

Solution-processed organic solar cells (OSCs) fabricated using versatile printing techniques such as the doctor blade, inkjet, and roll-to-roll methods offer advantages such as low cost, light weight, and solution processability.[1-5] Over the last few years, enormous efforts have been made to improve device performance, striving to achieve a power conversion efficiency (PCE) of 10% through the following strategies: 1) development of photoactive materials such as π-conjugated semiconducting polymer and fullerene derivatives, 2) utilization of functional layers for buffering, charge transportation, optical spacing, *etc*., and 3) modification of the morphology of photoactive films by post-annealing, solvent drying, or adding processing additives.[6-18] One of the most promising outcome of the these strategies is the use of low-bandgap semiconducting polymers comprising thieno[3,4-*b*]thiophene and benzodithiophene (poly(thieno[3,4-*b*]thiophene-alt-benzodithiophene) (PTB) series) in bulk-heterojunction (BHJ) OSCs. The BHJ OSCs were fabricated using [6,6]-phenyl-C$_{(61 \text{ or } 71)}$-butyric acid methyl ester (PC$_{(61 \text{ or } 71)}$BM) and achieved PCEs of up to 7.4%.[9] The development of semiconducting polymers with new structures has contributed to the production of materials that show PCEs exceeding 8% in OSCs,[19] making them strong candidates for next-generation solar cells and placing them in the same league as inorganic thin-film solar cells as well as dye-sensitized solar cells (DSSCs). In the past few years, considerable research has been also focused on developing efficient small-molecule organic semiconductors to improve the performance of solution-processed small-molecule OSCs (SMOSCs), with the near-term goal of attaining a PCE comparable to that of polymer solar cells (PSCs).[20,21] Small-molecule organic semiconductor materials are more attractive than polymer-based materials for mass production because the latter suffer from poor reproducibility of weight-average molecular weight and polydispersity index, among other characteristics, and are difficult to purify. Recently, SMOSCs with PCEs exceeding 6% have been reported, thus making solution-processed SMOSCs strong competitors to PSCs.[22]

The most commonly reported organic semiconductors for use in SMOSCs often have push-pull molecular skeletons composed of electron-donating groups (such as oligothiophene, bridged dithiophene, or triarylamine) bridged with electron-accepting groups (such as benzothiadiazole (BT), squaraine (SQ), diketopyrrolopyrrole (DPP), or methylene malononitrile) *via* π-conjugated motifs.[23-25] Recently, we reported several symmetric and unsymmetrical push-pull organic semiconductors containing various donors and acceptors for solution-processed SMOSCs.[26-36] The use of a triarylamine donor substantially stabilized separated holes from excitons, thereby improving the hole carrier transport properties of the material.[37-41] Notably, the use of the MMN acceptor unit increased the open-circuit voltage of the SMOSCs tested.[33-37] In addition, these push-pull structures in SMOSCs enabled efficient intramolecular charge transfer (ICT) to yield better molar absorptivity and a low bandgap. Thus inspired, we investigated the effects of π-conjugation length and planar rigidity of the bridging units, which can affect inter- and intramolecular CT, in these organic semiconductors.

Herein, we report the synthesis of three push-pull organic semiconductors, 2-((5"-(4-(diphenylamino)phenyl)-2,2';5',2"-terthiophene-5-yl)methylene)malononitrile (**TPA-Th$_3$-MMN**, **1**), 2-(5'-[5-(4-(diphenylamino)phenyl)-thiophene-2-yl]-thieno[3,2-*b*]thiophene-5-yl)methylene)malononitrile (**TPA-ThTT-MMN**, **2**), and 2-(5"-[5-(4-(diphenylamino)phenyl)-thiophene-2-yl]-dithieno[3,2-*b*:2,3-*d*]thiophene-5-yl)methylene)malononitrile (**TPA-ThDTT-MMN**, **3**), which are composed of triphenylamine (TPA) donors and MMN

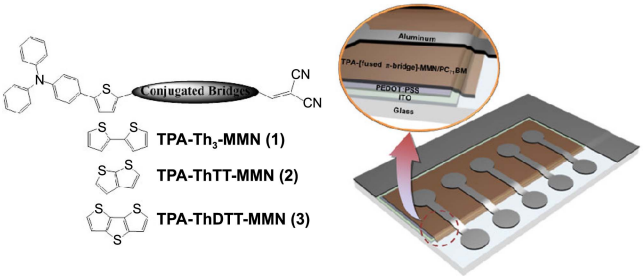

Scheme 1. Molecular structures of new synthetic organic semiconductors, **TPA-[π-bridges]-MMN** [**1**, **2**, and **3**] and device architecture of solution processed small molecule organic solar cell.

acceptors linked by various π-conjugated thiophene units to yield p-type organic semiconductors. We investigated the effects of the π-conjugated bridging unit on the photovoltaic characteristics in solution-processed SMOSCs (Scheme 1).

Experimental

General Method. Solvents were distilled from the appropriate reagents. All the reagents were purchased from Sigma-Aldrich, TCI, and Alfa Aesar. All reactions were carried out under nitrogen atmosphere. $PC_{71}BM$ was obtained from Nano-C. ^{1}H NMR, ^{13}C NMR, and ^{19}F NMR spectra were recorded using a Varian Mercury 300 spectrometer. Elemental analyses were performed with a Carlo Elba Instruments CHNS-O EA 1108 analyzer. Mass spectra were recorded using a JEOL JMS-SX102A instrument. Absorption and photoluminescence spectra were recorded using a Perkin-Elmer Lambda 2S UV-visible spectrometer and a Perkin LS fluorescence spectrometer, respectively. Cyclic voltammetry (CV) was carried out with a BAS 100B apparatus (Bioanalytical Systems, Inc.). A three-electrode system consisting of a non-aqueous reference electrode (0.1 M Ag/Ag^+ acetonitrile solution; MF-2062, Bioanalytical System, Inc.), a platinum working electrode (MF-2013, Bioanalytical System, Inc.), and a platinum wire (diam. 1.0 mm, 99.9% trace metals basis, Sigma-Aldrich) counter electrode was used. Redox potential measurements were performed in 0.1 M $(n\text{-}C_4H_9)_4N\text{-}PF_6$ in dichloromethane at a scan rate of 100 $mV{\cdot}s^{-1}$ (*vs*. external ferrocene/ferrocenium (Fc/Fc^+) reference). The thicknesses of organic layers were measured by alpha-step 250 surface profilometer (Tenco Instruments). Current-voltage (*J-V*) measurements were performed under simulated 100 $mW{\cdot}cm^{-2}$ AM 1.5G irradiation from a 1000 W Xe arc lamp (Oriel 91193). The light intensity was adjusted using a Si solar cell that was double-checked with a National Renewable Energy Laboratory (NREL)-calibrated Si solar cell (PV Measurements Inc.). The applied potential and cell currents were measured using a Keithley model 2400 digital source meter. The incident photon-to-current conversion efficiency (IPCE) spectra for the cells were recorded using an IPCE measuring system (PV Measurements Inc.).

Fabrication of Solar Cell Devices. The BHJ films were prepared under optimized conditions according to a previously reported protocol.[35] Indium tin oxide (ITO)-coated glass substrates were cleaned with detergent, ultrasonicated in acetone and isopropyl alcohol, and subsequently dried overnight in an oven. An aqueous solution of PEDOT:PSS (Heraeus, Clevios P VP.AI 4083) was spin-cast on the ITO substrates to obtain a 35 nm-thick film. The substrate was dried for 10 min at 140 °C in air and then transferred to a glove box before spin-casting the photoactive layer. Each of the synthesized organic semiconductors, were combined with $PC_{71}BM$ blend in several ratios (1:1-1:4 w/w) in chlorobenzene at a concentration of 30 mg/mL. The blends were spin-cast on the PEDOT layer, and the substrate was dried for 10 min at 80 °C in air. The TiO_x solution was spin-cast on the semiconducting photoactive layer, in air, to obtain a 10-nm-thick layer. Subsequently, the films were heated to 80 °C for 10 min in air. Finally, a ~100-nm-thick Al electrode was deposited on the BJH film under reduced pressure ($< 10^{-7}$ Torr).

Preparation of TiO_x Optical Spacer. The TiO_x material was prepared according to a previously reported procedure.[13] Titanium (IV) isopropoxide (10 mL) was added dropwise to a solution containing 2-methoxyethanol (50 mL) and ethanolamine (5 mL) under argon atmosphere. The solution was subjected to two cycles of heating: 80 °C for 2 h, then 120 °C for 1 h. The resulting dense TiO_x solution was diluted with isopropyl alcohol to prepare the typical TiO_x precursor solution.

Synthesis of 5-(4-(Diphenylamino)phenyl)-2,2';5',2''-terthiophene (v). Under nitrogen atmosphere, the mixture of compound **i** (3.9 g, 9.59 mmol), **ii** (3.56 g, 11.5 mmol), 2 M solution of K_2CO_3 (5.3 g, 38.39 mmol) in H_2O (20 mL), $Pd(PPh_3)_4$ (0.6 g, 0.47 mmol) in dry THF was refluxed at 80 ºC for 48 h. After cooling the solution, the organic layer was removed in vacuo. Then, the reaction was quenched with water. The solution was extracted with methylene chloride, dried with $MgSO_4$ and subjected to silica gel column chromatography (CH_2Cl_2/hexane = 1:4). Yield: 70%. mp 178-179 ºC. Mass: *m/z* 491.08 [M^+]. ^{1}H NMR (300 MHz, $CDCl_3$) δ 7.46 (d, 2H, *J* = 8.4 Hz), 7.29-7.21 (m, 11H), 7.10 (d, 2H, *J* = 7.8 Hz), 7.05 (t, 2H, *J* = 5.1 Hz), 7.00 (d, 4H, *J* = 6.9 Hz). ^{13}C-NMR (75 MHz, DMSO-d_6) δ 136.42, 136.02, 134.39, 134.15, 129.67, 128.46, 126.51, 126.37, 126.19, 125.42, 124.38, 124.26.

Synthesis of 5-[5-(4-(Diphenylamino)phenyl)-thiophene-2-yl]-thieno[3,2-*b*]thiophene (vi). The product **vi** was prepared using the same procedure of **v** except that the **iii** was used instead of the compound **ii**. Yield: 65%. mp 165-167 ºC. Mass: *m/z* 465.07 [M^+]. ^{1}H NMR (300 MHz, $CDCl_3$) δ 7.42 (d, 2H, *J* = 8.7 Hz), 7.31 (d, 1H, *J* = 3.3 Hz), 7.23 (t, 7H, *J* = 7.5 Hz), 7.18 (d, 1H, *J* = 5.1 Hz), 7.10 (d, 4H, *J* = 7.8 Hz), 7.01 (t, 4H, *J* = 8.4 Hz). ^{13}C NMR (75 MHz, DMSO-d_6) δ 139.57, 138.04, 137.40, 135.13, 129.67, 128.63, 127.02, 126.39, 125.40, 124.37, 123.80, 123.53, 122.91, 120.06.

Synthesis of 5-[5-(4-(Diphenylamino)phenyl)-thiophene-2-yl]-dithieno[3,2-*b*:2,3-*d*]thiophene (vii). The product **vii** was prepared using the same procedure of **v** except that the

iv was used instead of the compound **ii**. Yield: 85%. mp 170-171 ºC. Mass: *m/z* 521.74 [M^+]. ^{1}H NMR (300 MHz, $CDCl_3$) δ 7.42 (d, 2H, *J* = 8.4 Hz), 7.32 (d, 1H, *J* = 5.1 Hz), 7.29-7.23 (m, 8H), 7.14-7.01 (m, 8H). ^{13}C NMR (75 MHz, DMSO-d_6) δ 141.93, 141.17, 136.97, 136.83, 135.73, 129.66, 128.40, 128.36, 126.96, 126.41, 124.38, 123.91, 123.54, 122.86, 121.50.

Synthesis of 5''-(4-(Diphenylamino)phenyl)-2,2';5',2''-terthiophen-5-yl carbaldehyde (viii). Under nitrogen atmosphere and at 0 ºC, the $POCl_3$ (0.47 mL, 5.13 mmol) was dropwised in the mixture of compound **v** (2 g, 4.28 mmol) and DMF (3.32 mL, 42.85 mmol) in CH_2Cl_2 (50 mL), then was refluxed at 90 ºC for 24 h. After cooling the solution, the organic layer was removed in vacuo. Then, the reaction was quenched with 1 N NaOH solution. The solution was extracted with methylene chloride, dried with $MgSO_4$ and subjected to silica gel column chromatography (CH_2Cl_2/hexane = 1:1). Yield: 80%. mp 130-131 ºC. Mass: *m/z* 519.08 [M^+]. ^{1}H NMR (300 MHz, $CDCl_3$) δ 9.86 (s, 1H), 7.67 (d, 1H, *J* = 4.2 Hz), 7.44 (d, 2H, *J* = 8.7), 7.30-7.23 (m, 9H), 7.15 (t, 2H, *J* = 5.4 Hz), 7.11 (d, 4H, *J* = 6.9 Hz), 7.05 (d, 2H, *J* = 8.4 Hz). ^{13}C-NMR (75 MHz, DMSO-d_6) δ 146.73, 143.27, 141.21, 141.06, 139.31, 139.04, 138.14, 129.69, 126.46, 124.46, 124.00, 123.60, 122.57.

Synthesis of 5''-[5-(4-(Diphenylamino)phenyl)-thiophene-2-yl]-thieno[3,2-*b*]thiophene-5-yl carbaldehyde (ix). The product **ix** was prepared using the same procedure of **viii** except that the **vi** was used instead of the compound **v**. Yield: 60%. mp 148-149 ºC. Mass: *m/z* 493.06 [M^+]. ^{1}H NMR (300 MHz, $CDCl_3$) δ 9.92 (s, 1H), 7.86 (s, 1H), 7.44 (d, 2H, *J* = 8.4 Hz), 7.37 (s, 1H), 7.31-7.24 (m, 5H), 7.16 (d, 1H, *J* = 3.3 Hz), 7.11 (d, 2H, *J* = 8.4 Hz), 7.08-7.04 (m, 6H). ^{13}C NMR (75 MHz, DMSO-d_6) δ 178.23, 146.99, 146.70, 144.60, 144.32, 144.09, 131.32, 129.70, 126.59, 125.51, 124.10, 123.67, 122.65.

Synthesis of 5''-[5-(4-(Diphenylamino)phenyl)-thiophene-2-yl]-dithieno[3,2-*b*:2,3-*d*]thiophene-5-yl carbaldehyde (x). The product **x** was prepared using the same procedure of **viii** except that the **vii** was used instead of the compound **v**. Yield: 80%. mp 253-254 ºC. Mass: *m/z* 549.03 [M^+]. ^{1}H NMR (300 MHz, $CDCl_3$) δ 9.954 (s, 1H), 7.94 (s, 1H), 7.45 d, (2H, *J* = 8.4 Hz), 7.39 (s, 1H), 7.31-7.23 (m, 5H), 7.18-7.06 (m, 8H). ^{13}C NMR (75 MHz, DMSO-d_6) δ 178.23, 140.28, 139.43, 133.41, 132.96, 132.34, 131.77, 129.73, 128.16, 127.62, 124.37, 120.42, 120.04, 119.83, 118.41.

Synthesis of 2-((5''-(4-(Diphenylamino)phenyl)-2,2';5',2''-terthiophene-5-yl)methylene)malononitrile (TPA-Th$_3$-MMN, 1). Under nitrogen atmosphere, malononitrile (116.7 mg, 1.75 mmol) and piperidine (3-5 drops) were added to a solution of the carbaldehyde **viii** (91.1 mg, 1.75 mmol) in CH_2Cl_2 (20 mL) at room temperature. The reaction mixture was heated under reflux for 72 h. Then, the reaction was quenched with water. The solution was extracted with methylene chloride, dried with $MgSO_4$ and subjected to silica gel column chromatography (CH_2Cl_2/hexane = 3:1) to obtain the final product 2-((5''-(4-(diphenylamino)phenyl)-2,2';5',2''-terthiophene-5-yl)methylene)malononitrile (**1**). Yield: 56%. mp 163 ºC. Mass: *m/z* 567.09 [M^+]. ^{1}H NMR (300 MHz, $CDCl_3$) δ 7.74 (s, 1H), 7.61 (d, 2H, *J* = 4.2 Hz), 7.44 (d, 2H, *J* = 8.7 Hz), 7.35 (d, 2H, *J* = 4.2 Hz), 7.28 (d, 2H, *J* = 8.4 Hz), 7.19 (d, 2H, *J* = 4.5 Hz), 7.15 (t, 4H, *J* = 2.1 Hz), 7.11 (d, 4H, *J* = 8.4 Hz) 7.03 (t, 2H, *J* = 6.9 Hz). ^{13}C NMR (75 MHz, DMSO-d_6) δ 155.69, 146.63, 145.09, 142.77, 142.58, 142.00, 131.51, 129.89, 129.69, 129.56, 129.33, 124.58, 123.71, 111.47, 81.60.

Synthesis of 2-(5'-[5-(4-(diphenylamino)phenyl)-thiophene-2-yl]-thieno[3,2-*b*]thiophene-5-yl)methylene) malononitrile (TPA-ThTT-MMN, 2). The compound 2-(5'-[5-(4-(diphenylamino)phenyl)-thiophene-2-yl]-thieno[3,2-*b*]thiophene-5-yl)methylene)malononitrile (**2**) was prepared using the same procedure of **1** except that the **ix** was used instead of the compound **viii**. Yield: 50%. mp 167-168 ºC. Mass: *m/z* 541.07 [M^+]. ^{1}H NMR (300 MHz, $CDCl_3$) δ 7.85 (s, 1H), 7.79 (s, 1H), 7.31-7.28 (m, 5H), 7.18 (d, 1H, *J* = 3.3 Hz), 7.12 (d, 2H, *J* = 7.8 Hz), 7.09-7.05 (m, 6H). ^{13}C NMR (75 MHz, DMSO-d_6) δ 146.70, 142.58, 141.57, 140.68, 140.59, 139.34, 129.68, 129.34, 129.27, 128.03, 127.95, 126.90, 126.82, 126.68, 126.47, 124.49, 123.63, 81.50.

Synthesis of 2-(5''-[5-(4-(diphenylamino)phenyl)-thiophene-2-yl]-dithieno[3,2-*b*:2,3-*d*]thiophene-5-yl) methylene)malononitrile (TPA-ThDTT-MMN, 3). The compound 2-(5''-[5-(4-(diphenylamino)phenyl)-thiophene-2-yl]-dithieno-[3,2-*b*:2,3-d]thiophene-5-yl)methylene)malononitrile (**3**) was prepared using the same procedure of **1** except that the **x** was used instead of the compound **viii**. Yield: 53%. mp 251-252 ºC. Mass: *m/z* 597.05 [M^+]. ^{1}H NMR (300 MHz, $CDCl_3$) δ 7.90 (s, 1H), 7.81 (s, 1H), 7.45 (d, 2H, *J* = 8.4 Hz), 7.38 (s, 1H), 7.31-7.28 (m, 5H), 7.17 (d, 1H, *J* = 3.6 Hz), 7.12 (d, 2H, *J* = 7.8 Hz), 7.08-7.06 (m, 6H). ^{13}C NMR (75 MHz, DMSO-d_6) δ 158.47, 141.90, 136.85, 135.98, 135.72, 135.40, 129.70, 129.33, 129.30, 128.90, 124.77, 124.52, 124.19, 122.61, 122.05, 121.98, 121.77, 115.76, 80.64.

Results and Discussion

The synthetic methods used are outlined in Scheme 2. TPA-Th-Br **i** and the dioxaborolane derivatives of bithiophene, thienothiophene, and dithienothiophene (**ii-iv**) were prepared according to a modified procedure of procedure reported previously.[29] Suzuki coupling reactions of **i** and **ii** afforded **v**, which upon Vilsmeier-Haack reaction gave carbaldehyde **viii**. **TPA-Th$_3$-MMN** (**1**) was readily prepared in good yield (> 75%) through the Knoevenagel condensation of malononitrile and **viii**. **TPA-ThTT-MMN** (**2**) and **TPA-ThDTT-MMN** (**3**) were successfully synthesized from **ii** and **iii**, respectively, by the same method adopted for the synthesis of **TPA-Th$_3$-MMN**. The chemical structures of the synthesized products were verified by ^{1}H NMR, ^{13}C NMR, and matrix-assisted laser desorption ionization-time of flight (MALDI-TOF) mass analysis. These materials exhibited good solubility in common organic solvents such as dichloromethane, chloroform, chlorobenzene, and toluene.

Figure 1 shows the UV-visible absorption spectra of **1**, **2**, and **3** in chlorobenzene solution and in thin-film state; the

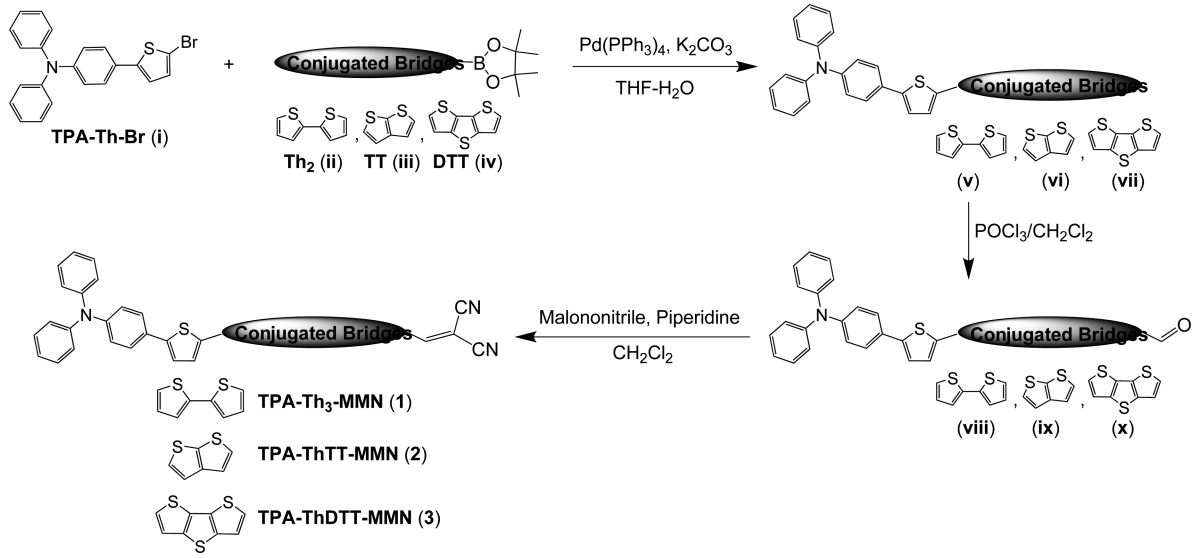

Scheme 2. Schematic depiction for the synthesis of the **TPA-[π-bridges]-MMN** [**1**, **2**, and **3**].

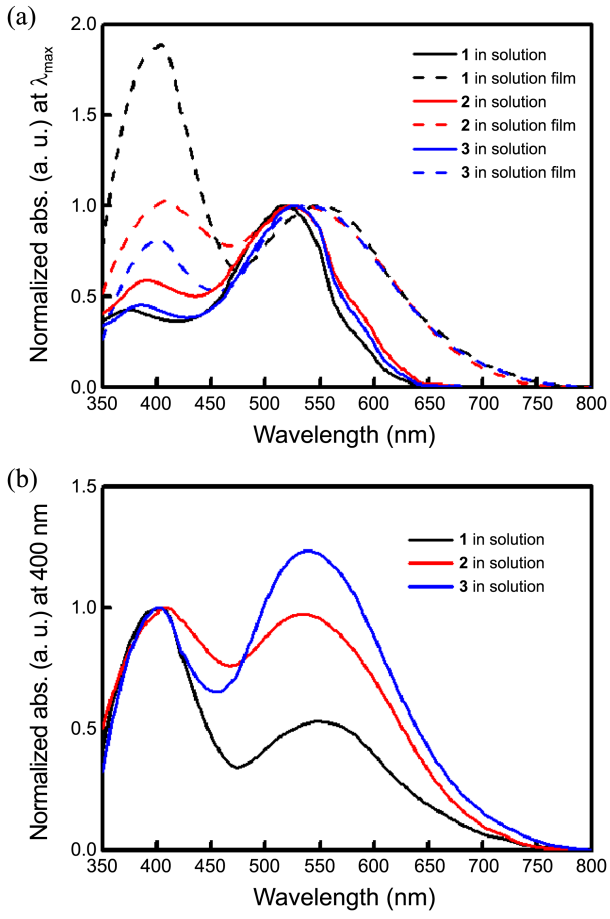

Figure 1. UV-Vis. absorption spectra of the **TPA-[π-bridges]-MMN** [**1** (black), **2** (red), and **3** (blue)] (a) normalized at λ_{max} in chlorobenzene solution (solid line) and thin films (dashed line) and (b) normalized at 400 nm in thin films.

corresponding optical properties are summarized in Table 1. The absorption spectra of **1** (black), **2** (blue), and **3** (red) in chlorobenzene (solid line) exhibited two typical transition bands in the 300-700 nm region. Molecular calculation by time dependent-density functional theory (TD-DFT) using the B3LYP functional/6-31G* basis set helped in further characterization of these transition bands (for details, see Figure S1 and Table S1 in Supporting Information). The absorption bands observed at longer wavelengths resulted from ICT monoexcitations originating in the highest occupied molecular orbital (HOMO) → lowest unoccupied molecular orbital (LUMO). The absorption bands observed at 300-500 nm were assignable to the π-π* transition, which predominantly originated from the HOMO-1 → LUMO excitation (f = 1.04-1.14) and exhibited intense oscillator strength (f) of transition. As shown in Figure 1(a) and Table 1, compounds **1**, **2**, and **3** in solution showed moderate molar absorption coefficients of 45,287 $M^{-1}\cdot cm^{-1}$ at 518 nm, 37,682 $M^{-1}\cdot cm^{-1}$ at 523 nm, and 51,507 $M^{-1}\cdot cm^{-1}$ at 527 nm, respectively, indicating a minor redshift of the absorption band due to the extended π-conjugation of the bridging units. In the thin-film state (Figure 1(b)), the absorption bands of **1**, **2**, and **3** showed a redshift relative to those in solution, and broader spectral peaks were observed. Interestingly, the absorption spectra normalized to the transition peak at 400 nm exhibited marked differences in the intensity of the absorption bands at longer wavelengths; this was particularly true for **3**, which had the DTT bridging unit. **2**, containing the TT bridging unit, also exhibited more intense absorption than did **1**. These results suggested that greater planarity and longer π-conjugation of the bridging units effectively facilitated intermolecular π-π packing interactions in the solid state.

Figure 2 shows the optimized structures of **1**, **2**, and **3** calculated by TD-DFT using the B3LYP functional/6-31G* basis set. The orbital densities of the LUMO of these molecules were predominantly located on the MMN accepting unit, while the orbital densities of the HOMO were located on the TPA-Th framework in **1** and **2** and on the TPA-Th-DTT framework in **3**, consistent with the general orbital distribution of push-pull organic semiconductors. These

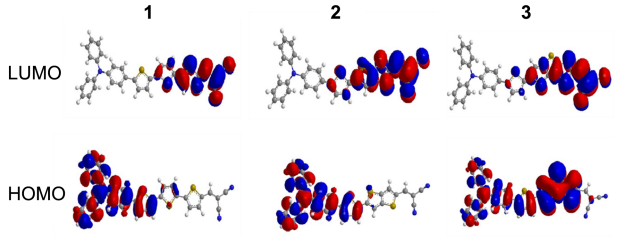

Figure 2. Isodensity surface plots of **TPA-[π-bridges]-MMN** [**1**, **2**, and **3**], calculated by the time dependent-density functional theory (TD-DFT) using the B3LYP functional/6-31G* basis set.

calculations revealed that absorption of photons induced efficient ICT from the TPA donor to the MMN acceptor and that DMM-TPA, in particular, served to stabilize separated electrons and holes and improve the transport properties of hole carriers such as the TPA donor.

Figure 3 shows the cyclic voltammograms of **1**, **2**, and **3** in methylene chloride; the corresponding electrochemical properties are summarized in Table 1. The HOMO and LUMO levels of these molecules were determined from CV spectra. A platinum rod electrode, a platinum wire, and a $Ag/AgNO_3$ (0.10 M) electrode were used as the working electrode, counter electrode, and reference electrode, respectively. The analyses were performed in an electrolyte solution of 0.1 M tetrabutylammonium hexafluorophosphate ($TBAPF_6$) in chloroform at room temperature under nitrogen, at a scan rate of 100 $mV{\cdot}s^{-1}$, using a ferrocenium/ferrocene redox couple as an external reference.

The HOMO and LUMO levels were deduced from the oxidation and reduction onsets under the assumption that the energy level of ferrocene (Fc) was 4.8 eV below vacuum level.[42,43] The cyclic voltammograms of these materials in solid-state thin films could not be measured owing to the stripping of the film from the electrode, and therefore, the bandgaps were determined from the solution-state voltammograms. The HOMO levels of **1**, **2**, and **3** were calculated as

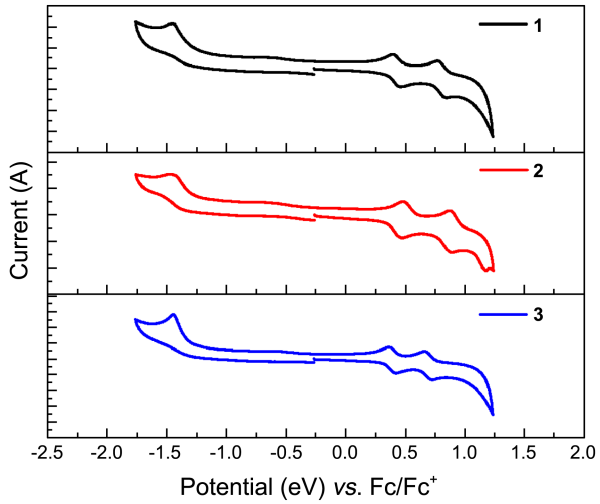

Figure 3. Electrochemical characterization of the **TPA-[π-bridges]-MMN** [**1** (black), **2** (red), and **3** (blue)] in dichloromethane/TBAHFP (0.1 M), scan speed 100 mV/s, potentials *vs.* Fc/Fc^+.

Table 1. Optical and electrochemical properties of **TPA-[π-bridges]-MMN** [**1**, **2**, and **3**]

Mat.	λ_{abs}[a]/nm ($\varepsilon/M^{-1}cm^{-1}$)	$E_{onset,\ ox}$ (V)/ HOMO (eV)[b]	$E_{onset,\ red}$ (V)/ LUMO (eV)[b]	E_{onset} (eV)[c]	$E_{0\text{-}0}$ (eV)[d]
1	391(18,070), 518(45,287)	0.353/ -5.153	-1.290/ -3.510	1.64	2.03
2	375(20,317), 523(37,682)	0.354/ -5.154	-1.300/ -3.500	1.65	1.96
3	386(23,250), 527(51,507)	0.330/ -5.130	-1.334/ -3.466	1.66	1.98

[a]Absorption spectra were measured in chlorobenzene solution. [b]Redox potential of the compounds were measured in CH_2Cl_2 with 0.1 M $(n\text{-}C_4H_9)_4NPF_6$ with a scan rate of 100 mVs^{-1} (*vs.* Fc/Fc^+). [c]E_{onset} was calculated by LUMO-HOMO. [d]$E_{0\text{-}0}$ was calculated from the absorption thresholds from absorption spectra in chlorobenzene solution.

5.148, 5.147, and 5.118 eV, respectively. The corresponding LUMO levels were 3.556, 3.527, and 3.513 eV, respectively. These results indicated that a greater planarity and longer π-conjugation of the bridging unit slightly increased the HOMO and slightly decreased the LUMO levels of the organic semiconductors.

Figure 4(a) shows the UV-visible absorption spectra of **1**/$PC_{71}BM$ (black), **2**/$PC_{71}BM$ (blue), and **3**/$PC_{71}BM$ (red) films, which exhibited the best performance in BHJ solar cell devices. The normalized absorption bands observed in these BHJ films nearly overlapped one another, indicating that the films exhibited similar spectral characteristics. To investigate the space-charge effects, we extracted the hole mobilities of the organic semiconductors from the space charge limitation of current (*SCLC*) *J-V* characteristics obtained in the dark for hole-only devices. Figure 4(b) shows the dark-current characteristics of ITO/PEDOT:PSS/**Donor**:$PC_{71}BM$/Au devices as a function of the bias, corrected by the built-in voltage determined from the difference in work function between Au and the PEDOT:PSS coated ITO. Ohm's law manifests at low voltages as an effect of thermal free carriers. In the presence of carrier traps in the active layer, a trap-filled limit (TFL) region exists between the ohmic and trap-free *SCLC* regions. *SCLC* behavior in the trap-free region can be characterized using the Mott-Gurney square law (1):[44]

$$J=(9/8)\varepsilon{\cdot}\mu(V2/L3) \quad (1)$$

where ε is the static dielectric constant of the medium and μ is the carrier mobility. The hole mobilities of **1**, **2**, and **3** evaluated using the above Mott-Gurney law ($\varepsilon = 3\varepsilon_0$) were 1.21×10^{-5}, 2.58×10^{-5}, and 1.48×10^{-5} $cm^2\ V^{-1}{\cdot}s^{-1}$, respectively. **2** and **3** exhibited slightly higher hole mobilities than did **1**. Specifically, the hole mobility of **2** was ~2 times that of **1**. These results showed that greater planarity resulted in enhanced hole transport properties *via* efficient intermolecular π-π packing interactions even in a BHJ system with $PC_{71}BM$.

These molecules were used for the fabrication of photovoltaic devices with PCBM BHJ films, and their performance

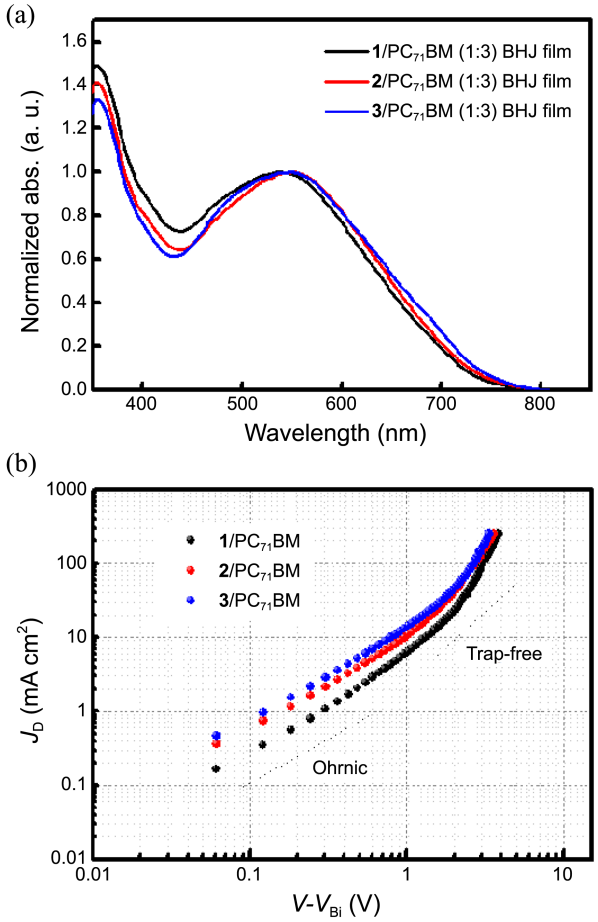

Figure 4. (a) UV-vis absorption spectra and (b) space charge limitation of current *J-V* characteristics of the **TPA-[π-bridges]-MMN** [**1** (black), **2** (red), and **3** (blue)]/$PC_{71}BM$ BHJ films, which hole-only devices (ITO/PEDOT:PSS/**Donor**:C_{71}-PCBM/Au).

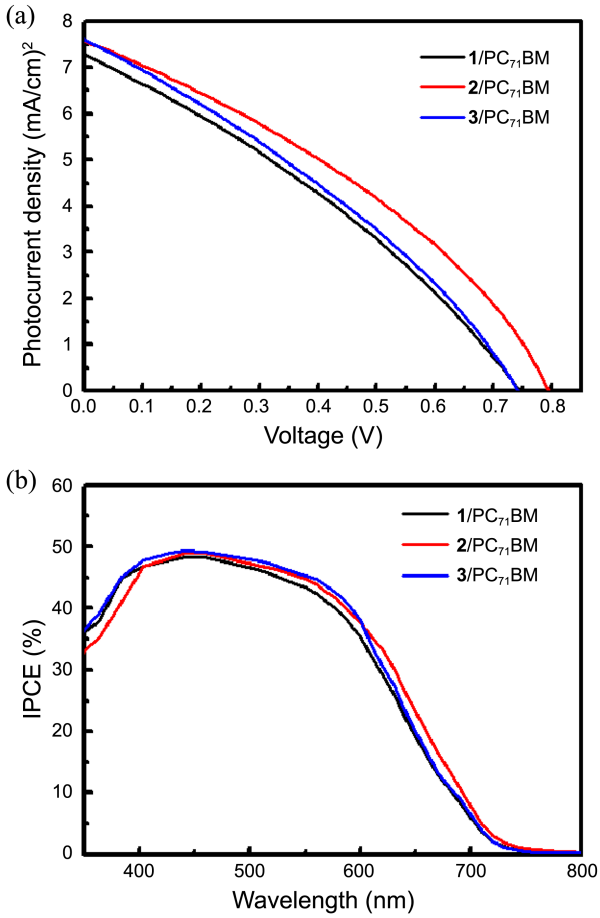

Figure 5. (a) Current (*J*)-voltage (*V*) curves under AM 1.5 conditions (100 mW/cm^2) and (b) IPCE spectra of the **TPA-[π-bridges]-MMN** [**1** (black), **2** (red), and **3** (blue)]/$PC_{71}BM$ BHJ solar cells fabricated under optimized processing condition with insertion of TiO_x layer.

was assessed. After studying the characteristics of more than 200 solar cells, we determined that the most efficient photovoltaic cells were obtained from the BHJ system fabricated using **1**, **2**, or **3** with $PC_{71}BM$, which were optimized at a ratio of 1:3. These BHJ films were cast on top of a PEDOT:PSS (Heraeus, AI 4083) layer. The optimum thicknesses of **1**/$PC_{71}BM$, **2**/$PC_{71}BM$, and **3**/$PC_{71}BM$ BHJ films obtained under these conditions were approximately 88, 93, and 76 nm, respectively. Figure 5 shows (a) the current-voltage (*J-V*) curves under AM 1.5 irradiation (100 mW·cm^{-2}) and (b) IPCE spectra of the organic semiconductor/$PC_{71}BM$ BHJ solar cells fabricated under optimized processing conditions with the insertion of TiO_x, which acts as an optical spacerand buffer layer,[13-14,34] between the photoactive layer and the Al electrode.

The corresponding values are summarized in Table 2. The IPCE spectra of these devices, as shown in Figure 5(b), revealed that the curves were well-matched with their optical absorptions, resulting in the close correlation with their photocurrents in the *J-V* curves. **2** exhibited a rather high photocurrent response at longer wavelengths as compared with **1** and **3**. As shown in Figure 5 and Table 2, conventionally fabricated devices with **1**/$PC_{71}BM$, **2**/$PC_{71}BM$, and **3**/$PC_{71}BM$ exhibited the following characteristics: PCE of 1.72% (± 0.13) with a short-circuit current (J_{sc}) of 7.28 mA·cm^{-2}, a fill factor (*F.F*) of 0.32, and V_{oc} of 0.74 V; a PCE of 2.09% (± 0.15) with J_{sc} = 7.58 mA·cm^{-2}, *F.F* = 0.35, and V_{oc} = 0.80 V; and a PCE of 1.80% (± 0.12) with J_{sc} = 7.60 mA·cm^{-2}, *F.F* = 0.31, and V_{oc} = 0.74 V, respectively. These results indicate that the greater planarity and longer π-conjugation of the bridging units in the skeletons of **2** and **3** led to the increased J_{sc} values of the SMOSCs fabricated with BHJ films made from these small molecules. In

Table 2. Photovoltaic performances of the devices fabricated with the **TPA-[π-bridges]-MMN** [**1**, **2**, and **3**]/$PC_{71}BM$ BHJ films[a]

Mat.	J_{sc} (mA·cm^{-2})	V_{oc}(V)	*F.F*	η (%)
1	7.28	0.74	0.32	1.72 ± 0.13
2	7.58	0.80	0.35	2.09 ± 0.15
3	7.60	0.74	0.31	1.80 ± 0.12

[a]The photovoltaic characteristics are performed under simulated 100 mW/cm^2 AM 1.5G illumination. The light intensity using calibrated standard silicon solar cells with a proactive window made from KG5 filter glass traced to the National Renewable Energy Laboratory (NREL). The masked active area of device is 4 mm^2.

particular, the best PCE was obtained for devices fabricated using the **2**/$PC_{71}BM$ film, which exhibited enhanced V_{oc} values. From these results, we observed that the organic semiconductors having more rigid and planar bridging motif exhibited rather red-shifted absorption spectra in BHJ composite film, resulting in the better quantum efficiency in longer wavelength region. However, we are still unable to explain the reason for the increased V_{oc} in devices fabricated using the **2**/$PC_{71}BM$ film.

Conclusion

We have demonstrated the synthesis of three push-pull organic semiconductors, **TPA-Th_3-MMN** (**1**), **TPA-ThTT-MMN** (**2**), and **TPA-ThDTT-MMN** (**3**), composed of TPA donors and MMN acceptors linked by various π-conjugated thiophene units to yield p-type organic semiconductors. We investigated the effects of the π-conjugated bridging unit on he photovoltaic characteristics of solution-processed SMOSCs fabricated using these molecules. Bridging units with greater planarity and longer π-conjugation facilitated intermolecular π-π packing interactions in the solid state and slightly increased the HOMO and decreased the LUMO levels of the organic semiconductors; this resulted in enhanced J_{sc} values of the SMOSCs fabricated with BHJ films made from **2** and **3**, which featured more planar and longer π-conjugated bridging units as compared to **1**. These results might serve as an important guide for developing novel materials and improving the performance of solution-processed SMOSCs using efficient functional layers.

Acknowledgments. This study was supported by research fund from Chosun University, 2012.

References

1. Krebs, F. C. *Sol. Energy Mater. Sol. Cells* **2009**, *93*, 394.
2. Dennler, G.; Scharber, M. C.; Brabec, C. J. *Adv. Mater.* **2009**, *21*, 1323.
3. Arias, A. C.; Mackenzie, J. D.; McCulloch, I.; Rivnay, J.; Salleo, A. *Chem. Rev.* **2010**, *110*, 3.
4. Krebs, F. C.; Fyenbo, J.; Tanenbaum, D. M.; Gevorgyan, S. A.; Andriessen, R.; van Remoortere, B.; Galagan, Y.; Jorgensen, M. *Energy Environ. Sci.* **2011**, *4*, 4116.
5. Nielsen, T. D.; Cruickshank, C.; Foged, S.; Thorsen, J.; Kreb, F. C. *Sol. Energy Mat. Sol. Cells* **2010**, *94*, 1553.
6. Hoppe, H.; Sariciftci, N. S. *J. Mater. Chem.* **2006**, *16*, 45.
7. Helgesen, M.; Søndergaard, R.; Krebs, F. C. *J. Mater. Chem.* **2010**, *20*, 36.
8. Park, S. H.; Roy, A.; Beaupre, S.; Cho, S.; Coates, N.; Moon, J. S.; Moses, D.; Leclerc, M.; Lee, K.; Heeger, A. J. *Nat. Photon.* **2009**, *3*, 297.
9. Price, S. C.; Stuart, A. C.; Yang, L.; Zhou, H.; You, W. *J. Am. Chem. Soc.* **2011**, *133*, 4625.
10. Zhou, H.; Yang, L.; Stuart, A. C.; Price, S. C.; Liu, S.; You, W. *Angew. Chem. Int. Ed.* **2011**, *50*, 2995.
11. Ma, W.; Yang, C.; Gong, X.; Lee, K.; Heeger, A. J. *Adv. Funct. Mater.* **2005**, *15*, 1617.
12. Yang, C.; Lee, J. K.; Heeger, A. J.; Wudl, F. *J. Mater. Chem.* **2009**, *19*, 5416.
13. Lee, K.; Kim, J. Y.; Park, S. H.; Kim, S. H.; Cho, S.; Heeger, A. J. *Adv. Mater.* **2007**, *19*, 2445.
14. Lee, J. K.; Coates, N. E.; Cho, S.; Cho, N. S.; Moses, D.; Bazan, G. C.; Lee, K.; Heeger, A. J. *Appl. Phys. Lett.* **2008**, *92*, 243308.
15. Lee, J. K.; Ma, W. L.; Brabec, C. J.; Yuen, J.; Moon, J. S.; Kim, J. Y.; Lee, K.; Bazan, G. C.; Heeger, A. J. *J. Am. Chem. Soc.* **2008**, *130*, 3619.
16. Kim, B.; Yeom, H. R.; Yun, M. H.; Kim, J. Y.; Yang, C. *Macromoleculs* **2012**, *45*, 8658.
17. Kim, B.; Yeom, H. R.; Choi, W. Y.; Kim, J. Y.; Yang, C. *Tetrahedron* **2012**, *68*, 6696.
18. Kim, G.; Yeom, H. R.; Cho, S.; Seo, J. H.; Kim, J. Y.; Yang. C. *Macromoleculs* **2012**, *45*, 1847.
19. Green, M. A.; Emery, K.; Hishikawa, Y.; Warta, W.; Dunlop, E. D. *Prog. Photovolt.* **2011**, *19*, 565.
20. Roncali, J. *Acc. Chem. Res.* **2009**, *42*, 1719.
21. Walker, B.; Kim, C.; Nguyen, T.-Q. *Chem. Mater.* **2011**, *23*, 470.
22. Sun, Y.; Welch, G. C.; Leong, W. L.; Takacs, C. J.; Bazan, G. C.; Heeger, A. J. *Nature Materials* **2012**, *11*, 44.
23. Tamayo, A. B.; Dang, X. D.; Walker, B.; Seo, J.; Kent, T.; Nguyen, T.-Q. *Appl. Phys. Lett.* **2009**, *94*, 103301.
24. Ma, C. Q.; Fonrodona, M.; Schikora, M. C.; Wienk, M. M.; Janssen, R. A. J.; Bauele, P. *Adv. Funct. Mater.* **2008**, *18*, 3323.
25. Ooi, Z. E.; Tam, T. L.; Shin, R. Y. C.; Chen, Z. K.; Kietzke, T.; Sellinger, A.; Baumgarten, M.; Mullen, K.; deMello, J. C. *J. Mater. Chem.* **2008**, *18*, 4619.
26. Jeong, B. S.; Choi, H.; Cho, N.; Ko, H. M.; Lim, W.; Song, K.; Lee, J. K.; Ko, J. *Sol. Energy Mat. Sol. Cells* **2011**, *95*, 1731.
27. So, S.; Choi, H.; Kim, C.; Cho, N.; Ko, H. M.; Lee, J. K.; Ko, J. *Sol. Energy Mat. Sol. Cells* **2011**, *95*, 3433.
28. So, S.; Choi, H.; Ko, H. M.; Kim, C.; Paek, S.; Cho, N.; Song, K.; Lee, J. K.; Ko, J. *Sol. Energy Mat. Sol. Cells* **2012**, *98*, 232.
29. Ko, H. M.; Choi, H.; Paek, S.; Kim, K.; Song, K.; Lee, J. K.; Ko, J. *J. Mater. Chem.* **2011**, *21*, 7248.
30. Cho, N.; Kim, J.; Lee, J. K.; Ko, J. *Tetrahedron* **2012**, *68*, 4029.
31. Kim, J.; Cho, N.; Ko, H. M.; Kim, C.; Lee, J. K.; Ko, J. *Sol. Energy Mat. Sol. Cells* **2012**, *102*, 159.
32. Choi, H.; Ko, H. M.; Cho, N.; Song, K.; Lee, J. K.; Ko, J. *ChemSusChem* **2012**, *5*, 2045.
33. Cho, N.; Song, K.; Lee, J. K.; Ko, J. *Chem. Eur. J.* **2012**, *18*, 11433.
34. Paek, S.; Cho, N.; Song, K.; Jun, M. J.; Lee, J. K.; Ko, J. *J. Phys. Chem. C* **2012**, *116*, 23202.
35. Lee, J. K.; Jeong, B. S.; Kim, J.; Kim, C.; Ko, J. *J. Photochem. Photobiol. A Chem.* **2012**, *251*, 25.
36. Paek, S.; Cho, N.; Cho, S.; Lee, J. K.; Ko, J. *Org. Lett.* **2012**, *14*, 6362.
37. Karpe, S.; Cravino, A.; Frère, P.; Allain, M.; Mabon, G.; Roncali, J. *Adv. Funct. Mater.* **2007**, *17*, 1163.
38. Roquet, S.; Cravino, A.; Leriche, P.; Alévêque, O.; Frére, P.; Roncali, J. *J. Am. Chem. Soc.* **2006**, *128*, 3459.
39. Cravino, A.; Leriche, P.; Aleveque, O.; Roquet, S.; Roncali, J. *Adv. Mater.* **2006**, *18*, 3033.
40. Wu, G.; Zhao, G.; He, C.; Zhang, J.; He, Q.; Chen, X.; Li, Y. *Sol. Energy Mat. Sol. Cells* **2009**, *93*, 108.
41. Leriche, P.; Frére, P.; Cravino, A.; Alévêque, O.; Roncali, J. *J. Org. Chem.* **2007**, *72*, 8332.
42. Pommerehene, J.; Vestweber, H.; Guss, W.; Mahrt, R. F.; Bässler, H.; Porsch, M.; Daub, J. *Adv. Mater.* **1995**, *7*, 551.
43. Chen, Z.; Debije, M. G.; Debaerdemaeker, T.; Osswald, P.; Würthner, F. *ChemPhysChem* **2004**, *5*, 137.
44. Mihalietchi, V. D.; Xie, H.; de Boer, B.; Koster, L. J. A.; Blom, P. W. M. *Adv. Funct. Mater.* **2006**, *16*, 669.